Electromagnetic Imaging for Inhomogeneous Dielectric Cylinder Buried in a Slab Medium

Chi-Hsien Sun, Ching-Lieh Li, Chien-Ching Chiu* and Chun Jen Lin

Electrical Engineering Department, Tamkang University, Tamsui, Taiwan 251, R.O.C.

Abstract

The electromagnetic imaging of inhomogeneous dielectric cylinders buried in a slab medium is investigated. Dielectric cylinders of unknown permittivities are buried in second space and scattered a group of unrelated waves incident from first space where the scattered field is recorded. By proper arrangement of the various unrelated incident field, the difficulties of ill-posedness and nonlinearity are circumvented, and the permittivity distribution can be reconstructed through simple matrix operations. The algorithm is based on the moment method and the unrelated illumination method. Numerical results are given to demonstrate the capability of the inverse algorithm. They also show that the permittivity distribution of the cylinders can be successfully reconstructed even when the permittivity is fairly large. Good reconstructed results are obtained even in the presence of additive Gaussian noise in measured data. In addition, the effect of noise on the reconstruction result is also investigated.

Key Words: Inverse Scattering, Unrelated Illumination Method, Dielectric Cylinder, Slab Medium, Microwave Imaging

1. Introduction

The electromagnetic imaging of objects buried in a slab medium has attracted because of its potential use in geophysical exploration and remote sensing. It also has been a subject of considerable importance in noninvasive measurement, medical imaging, and biological application. However, the solutions are considerably more difficult than those involving objects in a free space or half space. This is due to the interaction between the air-earth interface and the object, which leads to the complicated Green's function for this three layer problem. In the past, most of the research in the aspect emphasize on reconstruction of the second layer profile in the three layer structures [1–4]. However, the reconstruction of buried objects in the three structures is very sparse [5,6]. To the best of our knowledge, there is still no investigation on the electromagnetic imaging of inhomogeneous dielectric cylinders buried in a slab medium by the unrelated illumination method.

In this paper the electromagnetic imaging for inhomogeneous dielectric cylinders buried in a three layer structures is investigated. The algorithm is based on the moment method [7] and the unrelated illumination method [8]. In Section II, the theoretical formulation for electromagnetic imaging is presented. Numerical results for buried dielectric objects are given in Section III. Finally some conclusions are drawn in SectionIV.

2. Theoretical Formulation

Let us consider dielectric cylinders buried in a lossless homogeneous three-layer background as shown in Figure 1, where $(\varepsilon_i, \sigma_i)$ i = 1, 2, 3, denote the permittivities and conductivities in each region. The axis of the buried cylinder is the z axis; that is, the properties of the scatterer may vary with the transverse coordinates only. A group of unrelated incident waves with electric field

*Corresponding author. E-mail: djdeng@cc.ncue.edu.tw

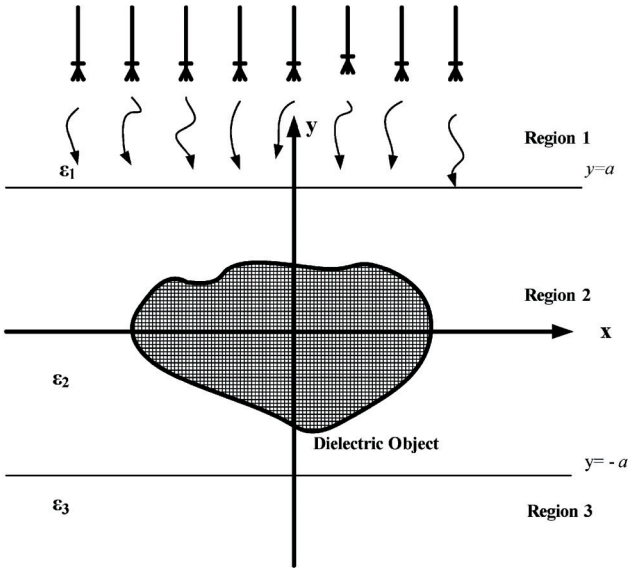

Figure 1. Geometry of the problem in (x,y) plane.

parallel to the z axis (i.e., transverse magnetic, or TM polarization) is illuminated upon the scatterers.

Owing to the interface, the incident plane wave generates three waves that would exist the absence of in the conducting object. Let the unperturbed field be represented by

$$\vec{E}^i(x,y)=\begin{cases}(E_z^i)_1(x,y)\hat{z}, & y\ge a,\\ (E_z^i)_2(x,y)\hat{z}, & a>y>-a,\\ (E_z^i)_3(x,y)\hat{z}, & y\le -a.\end{cases}$$

Then the internal total electric field inside the dielectric object, $\vec{E}(x,y)=E(x,y)\hat{z}=[E_z^i(x,y)+E_z^s(x,y)]\hat{z}$, can be expressed by the following integral equation:

$$E_z^i(\vec{r})=\int_s G(\vec{r},\vec{r}')k_2^2\left[\varepsilon_d(\vec{r}')-1\right]E_z(\vec{r}')ds'+E_z(\vec{r}),\quad a>y>-a \tag{1}$$

The scattered field, $\vec{E}_s(x,y)=E_z^s(x,y)\hat{z}$, can be expressed as

$$E_z^s(\vec{r})=-\int_s G(\vec{r},\vec{r}')k_2^2\left[\varepsilon_d(\vec{r}')-1\right]E_z(\vec{r}')ds' \tag{2}$$

with

$$G(x,y;x',y')=\begin{cases}G_{1s}(x,y:x',y'), & y\ge a,\\ G_{2s}(x,y;x',y'), & -a<y<a,\\ G_{3s}(x,y;x',y'), & y\le -a,\end{cases} \tag{3a}$$

where

$$G_{1s}(x,y;x',y')=\frac{1}{2\pi}\int_{-\infty}^{\infty}je^{-j\gamma_1(y-a)}\frac{(\gamma_2+\gamma_3)e^{j\gamma_2(y'+a)}+(\gamma_2-\gamma_3)e^{-j\gamma_2(y'+a)}}{(\gamma_1+\gamma_2)(\gamma_2+\gamma_3)e^{j\gamma_2(2a)}+(\gamma_1-\gamma_2)(\gamma_2-\gamma_3)e^{-j\gamma_2(2a)}}e^{-j\alpha(x-x')}d\alpha \tag{3b}$$

$$G_{2s}(x,y;x',y')=G_{2sf}(x,y;x',y')+G_{2ss}(x,y;x',y') \tag{3c}$$

$$G_{3s}(x,y;x',y')=\frac{1}{2\pi}\int_{-\infty}^{\infty}je^{j\gamma_1(y+a)}\frac{(\gamma_1+\gamma_2)e^{-j\gamma_2(y'-a)}+(\gamma_2-\gamma_1)e^{j\gamma_2(y'-a)}}{(\gamma_1+\gamma_2)(\gamma_2+\gamma_3)e^{j\gamma_2(2a)}+(\gamma_1-\gamma_2)(\gamma_2-\gamma_3)e^{-j\gamma_2(2a)}}e^{-j\alpha(x-x')}d\alpha \tag{3d}$$

where

$$G_{2sf}(x,y;x',y')=\frac{j}{4}H_0^{(2)}(k_2\sqrt{(x-x')^2+(y-y')^2})$$

$$G_{2ss}(x,y;x',y')=\frac{1}{2\pi}\int_{-\infty}^{\infty}\frac{j}{2\gamma_2}\left\{\left[\frac{(\gamma_2-\gamma_1)(\gamma_2-\gamma_3)\left[e^{-j\gamma_2[|y-y'|+2a]}+e^{j\gamma_2[|y-y'|-2a]}\right]}{(\gamma_1+\gamma_2)(\gamma_2+\gamma_3)e^{j\gamma_2(2a)}+(\gamma_1-\gamma_2)(\gamma_2-\gamma_3)e^{-j\gamma_2(2a)}}\right]+\left[\frac{(\gamma_2-\gamma_1)(\gamma_2+\gamma_3)e^{j\gamma_2(y+y')}+(\gamma_2-\gamma_3)(\gamma_1+\gamma_2)e^{-j\gamma_2(y+y')}}{(\gamma_1+\gamma_2)(\gamma_2+\gamma_3)e^{j\gamma_2(2a)}+(\gamma_1-\gamma_2)(\gamma_2-\gamma_3)e^{-j\gamma_2(2a)}}\right]\right\}e^{-j\alpha(x-x')}d\alpha$$

$\gamma_i^2=k_i^2-\alpha^2$, $i=1,2,3$, $\mathrm{Im}(\gamma_i)\le 0$, $-a<y'<a$.

Here k_i denotes the wave number in region i. $G(x, y; x', y')$ is the Green's function, which can be obtained by Fourier transform [9]. For numerical implementation of Green's function, we might face some difficulties in calculating this function. This Green's function is in the form of an improper integral, which must be evaluated numerically.

However, the integral converges very slowly when (x, y) and (x', y') approach the interface $y = a$. Fortunately we find that the integral in G_{1s}, G_{2s} and G_{3s} may be re-

written as a closed-form term plus a rapidly converging integral [10]. Thus the whole integral in the Green's function can be calculated efficiently.

The direct scattering problem is to calculate the scattered field E_z^s in Region 1, while the permittivity distribution of the buried objects is known. This can be achieved by first solving the internal total field E in Eq. (1) and calculating E_z^s in Eq. (2). For numerical implementation of the direct problem, the dielectric objects are divided into N sufficient small cells. Thus the permittivity and the total field within each cell can be taken as constants. Then the moment method is used to solve Eqs. (1) and (2) with a pulse basis function for expansion and point matching for testing [7].

For the inverse scattering problem, the permittivity distribution of the dielectric objects is to be computed by the knowledge of the scattered field measured in Region 1. In the inversion procedure, N different t column vectors are chosen to illuminate the objects, and the moment method is employed to transform Eqs. (1) and (2) into the following matrix equations:

$$[E_z^i] = \left[[G_2][\tau_d] + [I]\right][E_z] \tag{4}$$

$$[E_z^s] = -[G_1][\tau_d][E_z] \tag{5}$$

where $[E_z^i]$ and $[E_z]$ are $N \times N$ square matrices. $[E_z^s]$ is a $M \times N$ matrix. Here M is the number of measurement point. The matrices $[G_1]$ and $[G_2]$ are $M \times N$ and $N \times N$ matrices, respectively. The element in matrices $[G_1]$ and $[G_2]$ can be obtained by tedious mathematical manipulation. $[\tau_d]$ is a $N \times N$ diagonal matrix whose diagonal element $[\tau_d]_{nm}$ is equal to $[\varepsilon_{dn}]_{nm}$ minus 1. $[I]$ is a $N \times N$ identity matrix. The element in matrices $[G_i]$, i = 1, 2 can be obtained by tedious mathematic manipulation (see Appendix). If we solve $[E_z]$ in Eq. (4) and substitute into Eq. (5), then $[\tau_d]$ can be found by following equation:

$$[\Psi_b][\tau_d] = [\Phi_b] \tag{6}$$

where

$$[\Phi_b] = -[E_z^s][E_z^i]^{-1}$$

$$[\Psi_b] = [E_z^s][E_z^i]^{-1}[G_2] + [G_1]$$

From Eq. (6), all the diagonal matrix in matrix $[\tau_d]$ can be determined by comparing the element with the same subscripts, which may be any row of both $[\Phi_b]$ and $[\Psi_b]$. Then the permittivity of each cell, ε_n, can be obtained by $[\tau_d]_{nm} + 1$. Note that there are a total of M possible values for each element of $[\tau_d]$. Therefore, the average value of these M data is computed and chosen as the final reconstruction result in the simulation.

In the above derivation, the key problem is that the incident matrix $[E_z^i]$ must not be a singular matrix; that is, the entire incident column vectors that from the $[E_z^i]$ matrix, must be linearly unrelated. Thus, if the objects are illuminated by a group of unrelated incident waves, it is possible to reconstruct the permittivity distribution of the objects. Note that when the number of cells becomes very large, it is difficult to make such a great number of independent measurements. In such a case, some regularization methods must be used to overcome the ill-posedness.

3. Numerical Results

We illustrate the performance of the proposed inversion algorithm and its sensitivity to random noise in the scattered field. Consider a lossless three- layer structure ($\sigma_1 = \sigma_2 = \sigma_3 = 0$) and the width of the second layer is 0.2 m. The permittivity in each region is characterized by, $\varepsilon_1 = \varepsilon_0$, $\varepsilon_2 = 2.25\varepsilon_0$, and $\varepsilon_3 = \varepsilon_0$ respectively, as shown in Figure 1. The frequency of the incident wave is chosen as 3 GHz. The incident waves are generated by numerous groups of radiators operated simultaneously.

Each group of radiators is restricted to transmit a narrow-beamwidth pattern which can be implemented by antenna array techniques. By changing the beam direction and tuning the phase of each group of radiators, one can focus all the incident beams in turn at each cell of the object. This procedure is called beam focusing [8]. Note that this focusing should be set when the scatterer is absent. Cleary, an incident matrix formed in this way is diagonally dominant and its inverse matrix exists. The measurement is taken from 0.4 m to -0.4 m in region 1 at equal spacing. The number of measurement points is set to be 9 for each illumination. For avoiding trivial inversion of finite-dimensional problems, the discretization number for the direct problem is four times that for the inverse problem in our numerical simulation.

In the first example, a buried cylinder with a 50 mm × 10 mm rectangular cross section is discretized into 25 ×

5 cells, and their relative dielectric permittivities are plotted in Figure 2(a). Each cell has a 2 mm × 2 mm cross section. The reconstructed permittivity distribution is shown in Figure 2(b). The root-mean-square(RMS) error is about 1.3%. It is clear that the reconstruction is good.

In the second example, a buried cylinder with a 60 mm × 60 mm rectangular cross section is discretized into 20 × 20 cells, and their relative dielectric permittivities are plotted in Figure 3(a). Each cell has a 3 mm × 3 mm cross section. The reconstructed permittivity distribution is shown in Figure 3(b). The root-mean-square(RMS) error is about 0.5%. It is found that the reconstruction is good.

To investigate the effects of noise, we add to each complex scattered filed a quantity b + cj, where b and c are independent random numbers having a Gaussian distribution over 0 to the noise levels applied are times the rms value of the field. The noise levels applied 10^{-5}, 10^{-4}, 10^{-3}, 10^{-2} and 10^{-1} in the simulations. The numerical results for examples 1 and 2 are plotted in Figure 4. They show the effect of noise is tolerable for noise levels below 1%.

Our method depends on the condition number of $[E_z^i]$; that is, on having N unrelated measurements. The procedure will generally not work when the number of unknowns gets very large. This is due to the fact that it is difficult to make so many measurements and make them all unrelated. As a result, the condition number of $[E_z^i]$ will

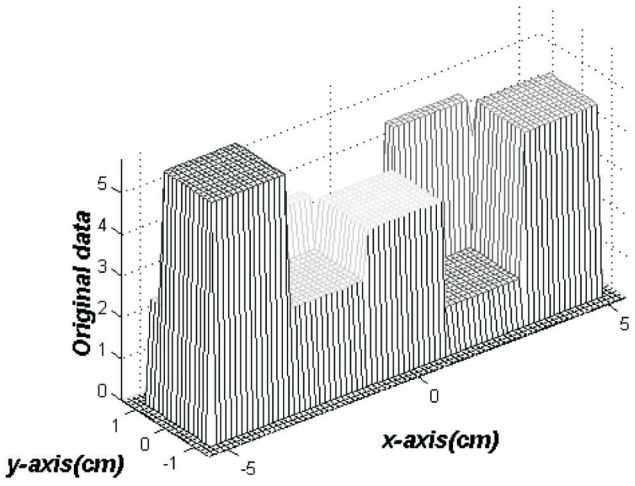

Figure 2(a). Original relative permittivity distribution of the dielectric cylinder for example 1.

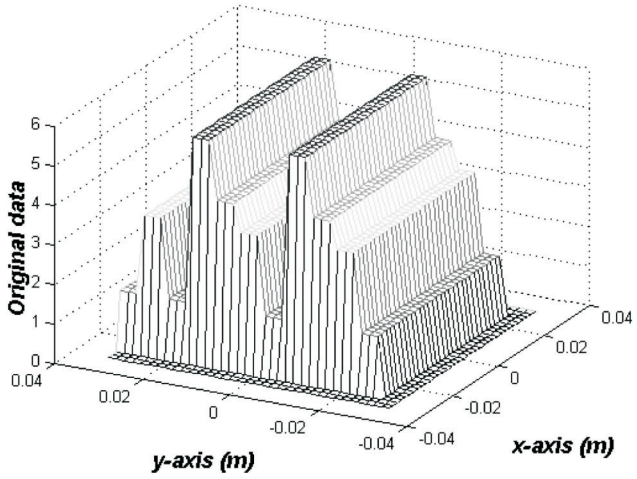

Figure 3(a). Original relative permittivity distribution of the dielectric cylinder for example 2.

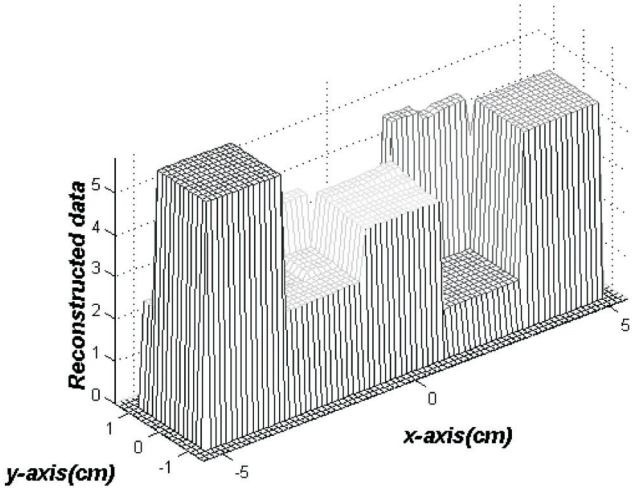

Figure 2(b). Reconstructed relative permittivity distribution of the dielectric cylinder for example 1.

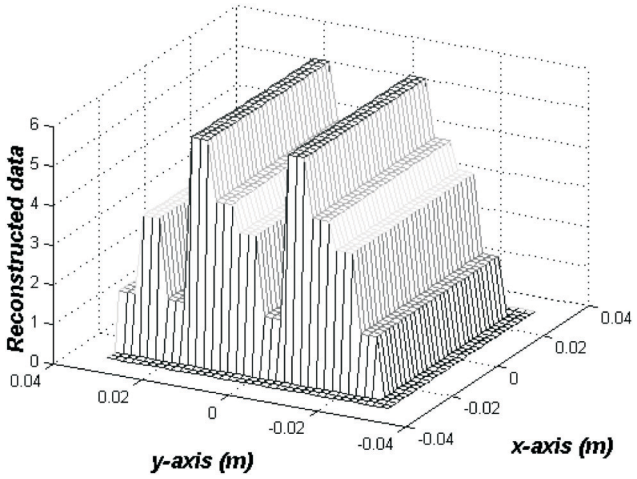

Figure 3(b). Reconstructed relative permittivity distribution of the dielectric cylinder for example 2.

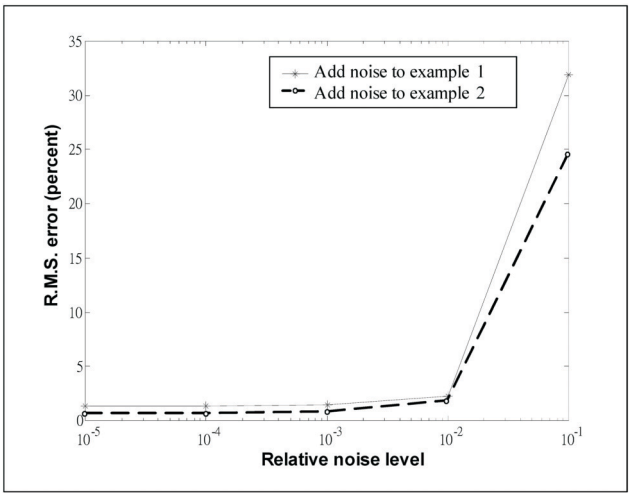

Figure 4. Reconstructed error as a function of the normalized standard deviation of Gaussian noise for example 1 and example 2.

become large when the number of unknowns is very large. In this case, the regularization method should be employed to overcome the ill-posedness. For instance, the pseudoinverse transform techniques [11] can be applied for the inversion of the $[E_z^i]$ matrix. For our experience, the regularization process is needed when the number of unknowns are more then 1000.

4. Conclusions

An efficient algorithm for reconstructing the permittivity distribution of dielectric cylinders buried in a three-layer space has been proposed. By properly arranging the direction of various unrelated waves, the difficulty of ill-posedness and nonlinearity is avoided. Thus, the permittivity distribution can be obtained by simple matrix operations. The moment method has been used to transform a set of integral equations into matrix form. Then these matrix equations are solved by the unrelated illumination method. Numerical simulation for imaging the permittivity distribution of a buried dielectric object has been carried out and good reconstruction has been obtained even in the presence of Gaussian noise in measured data. This algorithm is very effective and efficient, because no iteration is required.

APPENDIX

The element in the matrix $[G_1]$ can be written as

$$(G_1)_{mn} = \left[k_2^2 \cdot \iint_{cell\ n} G_{1s}(x, y; x', y')dx'dy' \right]\Bigg|_{\substack{x=x_m \\ y=y_m}}$$

where (x_m, y_m) is the observation point located in the center of the mth cell. For a sufficient small cell, we can replace the cell by a circular cell with the same cross section [12]. Let the equivalent radius of the nth circular cell be a_n. The $(G_1)_{mn}$ can be expressed in the following form

$$(G_1)_{mn} = G_{1s}(x_m, y_m; x_n, y_n) \cdot k_2^2 \cdot \Delta S_n$$

where (x_n, y_n) is the center of the cell n. ΔS_n denotes the area of the nth cell.
Similarly,

$$(G_2)_{mn} = \begin{cases} G_{2ss}(x_m, y_m; x_n, y_n) \cdot k_2^2 \cdot \Delta S_n \\ \quad + \dfrac{j\pi k_2 a_n}{2} J_1(k_2 a_n) H_0^{(2)}(k_2 \rho_{mn}), & m \neq n \\ G_{2ss}(x_m, y_m; x_n, y_n) \cdot k_2^2 \cdot \Delta S_n \\ \quad + \dfrac{j}{2}\left[\pi k_2 a_n H_1^{(2)}(k_2 a_n) - 2j \right] & m = n \end{cases}$$

where $\rho_{mn} = \sqrt{(x_m - x_n)^2 + (y_m - y_n)^2}$, J_1 is Bessel function of the first order.

References

[1] Omar, A. S. and Akhtar, M. J., "A Generalized Technique for the Reconstruction of Permittivity Profiles With a Controllable Resolution in an Arbitrary Coordinate System," *IEEE Transactions on Antennas and Propagation,* Vol. 53, pp. 294–304 (2005).

[2] Soldovieri, F. and Persico, R., "Reconstruction of an Embedded Slab from Multifrequency Scattered Field Data under the Distorted Born Approximation," *IEEE Transactions on Antennas and Propagation,* Vol. 52, pp. 2348–2356 (2004).

[3] Mikhnev, V. A. and Vainikainen, P., " Two-Step Inverse Scattering Method for One-Dimensional Permittivity Profiles," *IEEE Transactions on Antennas and Propagation,* Vol. 48, pp. 293–298 (2000).

[4] Nabulsi, K. A. and Dudley, D. G., "A New Approximation and a New Measurable Constraint for Slab Profile Inversion," *IEEE Transactions on Geoscience and Remote Sensing,* Vol. 34 (1996).

[5] Lin, Y. S., Chiu, C. C.,"Image Reconstruction for a Perfectly Conducting Cylinder Buried in Slab Medium by a TE Wave Illumination," *Electromagnetics,* pp. 203–216 (2005).

[6] Lin, C. J., Chou, C. Y. and Chiu, C. C., "Electromagnetic Imaging for a Conducting Cylinder Buried in a Slab Medium by the Genetic Algorithm," *International Journal of Imaging Systems and Technology,* Vol. 14 , pp. 1–7 (2004).

[7] Harrington, R. F., Field Computation by Moment Methods, Macmillan, New York (1968).

[8] Wang, W. and Zhang, S., "Unrelated Illumination Method for Electromagnetic Inverse Scattering of Inhomogeneous Lossy Dielectric Bodies," *IEEE Transactions on Antennas and Propagation,* Vol. AP-40, pp. 1292–1296 (1992).

[9] Wait, J. R., *Electromagnetic Waves in Stratified Media,* Macmillan, New York (1962).

[10] Chiu, C. C. and Kiang, Y. W., "Inverse Scattering of a Buried Conducting Cylinder," *Inv. Prob.,* Vol. 7, pp. 187–202 (1991).

[11] Ney, M. M., Smith, A. M. and Stuchly, S. S., "A Solution of Electromagnetic Imaging Using Pseudoinverse Transformation," *IEEE Trans. Med. Imag.,* Vol. MI-3, pp. 155–162 (1984).

[12] Richmond, J. H., "Scattering by a Dielectric Cylinder of Arbitrary Cross Section Shape," *IEEE Trans. Antennas Propagat.,* Vol. 13, pp. 334–341 (1965).

Manuscript Received: Nov. 8, 2007
Accepted: Jul. 24, 2008